JBC Papers in Press. Published on July 26, 2007 as Manuscript M701984200
The latest version is at http://www.jbc.org/cgi/doi/10.1074/jbc.M701984200

IMPACT OF TWO NOVEL MUTATIONS ON THE STRUCTURE AND FUNCTION OF HUMAN MYELOPEROXIDASE

Melissa Goedken[1], Sally McCormick[1], Kevin G. Leidal[1], Kazuo Suzuki[2], Yosuke Kameoka[3], Joshua M. Astern[4], Meilan Huang[5], Artem Cherkasov[5], William M. Nauseef [1]

[1]Inflammation Program, Department of Medicine, University of Iowa and Veterans Affairs Medical Center, Iowa City, IA 52241, [2]National Institute of Infectious Diseases, Toyama 1-23-1, Shinjuku-ku, Tokyo 162 8640, [3]Laboratory of Genetic Resources, Division of Biomedical Resources, National Institute of Biomedical Innovation 7-6-8, Saitoasagi, Ibaraki-city, Osaka, 567-0085, [4] University of North Carolina at Chapel Hill, UNC Kidney Center, 5009 Burnett-Womack Bldg, Chapel Hill, NC 27599, and [5]Division of Infectious Diseases, Department of Medicine, Faculty of Medicine, University of British Columbia.

Running title: Missense mutations in the heme pocket of myeloperoxidase

Address all correspondence to William M. Nauseef, Inflammation Program, and Department of Medicine, Roy J. and Lucille A. Carver College of Medicine, University of Iowa, D160 MTF, 2501 Crosspark Road, Coralville, IA, 52241, USA. Phone: 1-319-335-4278; Fax: 1-319-335-4194; Email: william-nauseef@uiowa.edu.

The heme protein myeloperoxidase (MPO) contributes critically to O_2-dependent neutrophil antimicrobial activity. Two Japanese adults were identified with inherited MPO deficiency due to mutations at R499 or G501, conserved residues near the proximal histidine in the heme pocket. Because of the proximity of these residues to a critical histidine in the heme pocket, we examined the biosynthesis, function, and spectral properties of the peroxidase stably expressed in HEK cells. Biosynthesis of normal MPO by HEK cells faithfully mirrored events previously identified in cells expressing endogenous MPO. Mutant apoproMPO was 90-kDa and interacted normally with the ER molecular chaperones ERp57, calreticulin, and calnexin. However, mutant precursors were not proteolytically processed into subunits of MPO, although secretion of the unprocessed precursors occurred normally. Although [^{14}C]-δ-aminolevulinic acid incorporation demonstrated formation of proMPO in both mutants, neither protein was enzymatically active. The Soret band for each mutant was shifted from the normal 430 nm to ~412 nm, confirming that heme was incorporated but suggesting that the number of covalent bonds or other structural aspects of the heme pocket were disrupted by the mutations. These studies demonstrate that despite heme incorporation, mutations in the heme environs compromised the oxidizing potential of MPO.

Phagocytes contribute significantly to human innate immunity and polymorphonuclear neutrophils (PMN) are the predominant granulocyte in the circulation. When PMN are deficient in number or function, normal antimicrobial action is severely compromised, resulting in increased morbidity and mortality from infection. Well suited for the wide diversity of potential microbial challenges, PMN possess a broad array of responses by which to contain, control, kill, and degrade microorganisms,

both in the phagosome and within the immediate cellular environs. These defenses include degradative and antimicrobial proteins, fabricated during myeloid development and stored within the granules, as well as reactive oxygen and nitrogen species generated *de novo* specifically in response to invasion. None of these elements functions alone but rather there is extensive and overlapping collaborations within the context of the phagosome.

The most extensively studied example of the synergistic antimicrobial systems within human PMN is the myeloperoxidase-H_2O_2-halide system (1). PMN simultaneously activate the normally dormant NADPH oxidase and release granule contents in response to stimulation. The H_2O_2 produced by the multicomponent phagocyte NADPH oxidase (2) converts the azurophilic granule protein myeloperoxidase (MPO) from its resting state into compound I, a transient intermediate with potent oxidizing properties, which in turn oxidizes Cl^- to Cl^+, thereby generating the potent antimicrobial agent HOCl (3). In addition to HOCl, chloramines and other longer-lived products of the MPO-H_2O_2-halide system have been implicated in mediating cytotoxicity to a broad array of microorganisms as well as mammalian proteins and cells (4-10). In its capacity as a peroxidase, the activity of MPO depends on a normal heme group, which in the case of MPO is a ferric protoporphyrin IX covalently linked to the protein backbone (11;12). Data from the crystal structure of native human MPO indicate that the heme group stably interacts with the protein backbone via three covalent bonds and eight hydrogen bonds (11). Structural features unique to the heme group of MPO make it the only member of the animal peroxidase family capable of oxidizing chloride and thus generating HOCl, at physiologic pH (13-15).

Significant insights into the normal biosynthesis, structure, and function of MPO have been derived from studies of the functional impact of inherited mutations (reviewed in 6)(16-20). To date, none of the previously characterized genotypes has directly involved the region around the heme group of MPO. However, missense mutations at residue 501[1] (glycine to serine, G501S) and residue 499 (arginine to cysteine, R499C) have been identified in two unrelated Japanese individuals with inherited MPO deficiency (21;22). We describe here the structural and functional consequences caused by G501S and R499C - two mutations adjacent to the critical histidine 502 on the proximal side of the heme in MPO.

EXPERIMENTAL PROCEDURES

Materials

K562 erythroleukemia cells and human embryonal kidney 293 (HEK) cells were obtained from American Type Culture Collection (Manassas, VA): ATCC CCL 243 and CRL-1573, respectively. Vectors pREP10 and pcDNA3.1 and antibiotics hygromycin and G-418 sulfate were obtained from Invitrogen (Carlsbad, CA); [^{35}S]-methionine/cysteine (26.7 x 10^7 Bq/0.5 ml) from Amersham Pharmacia Biotech (Piscataway, NJ). [^{14}C]-δ-aminolevulinic acid (45.7 mCi/mmol) was custom made by Perkin Elmer Life and Analytical Sciences (Boston, MA). All tissue culture reagents were obtained from University of Iowa Hybridoma Facility. Antibodies against calnexin and ERp57 were obtained from Stressgen Bioreagents (Ann Arbor, MI). The monospecific rabbit antibody against human myeloperoxidase was generated in our lab (23), as was the rabbit antibody against human calreticulin (24), the latter available commercially from Affinity Bioreagents (Golden, CO). Endoglycosidase H and N-glycosidase F from *Chryseobacterium meningosepticum* were obtained from Calbiochem (La Jolla, CA).

Unless otherwise specified, all other reagents were purchased from Sigma-Aldrich (St. Louis, MO).

Molecular Modeling

Reasoning that the missense mutations at residues 499 and 501 might adversely influence the structure around the heme in MPO, we modeled the active site of native and

mutant forms of the protein. To that end, the three-dimensional structure of human MPO protein was retrieved from the protein database (PDB code:1D2V[3]) and its heme-containing domain was subjected to simplistic energy minimization. For all three structures, we performed force-field based energy minimization of side chains in proximity to the heme in order to gain insight into the geometry and possible conformational changes of critical residues at the atomic level. We considered the heme, iron, and bromide ions and close-proximity residues (Figure 1). Mutant MPO structures were derived from the native MPO crystal structure by the *in silico* replacement of Arg 499 with cysteine and Gly 501 with serine using a molecular modeling package (Molecular Operation Environment. V. 2004.10, Chemical Computation Group, Montreal, 2005). The geometry of introduced residues of the mutant forms in the active site was minimized using the CHARMM 22 force field (25). The hydrogen atoms were added to the structures of native and mutated MPO protein using CHARMM HBUILD module and their positions were further optimized.

Stably transfected cells lines

K562 erythroleukemia cells were maintained in 1640 RPMI with 10% fetal calf serum, 2 mM L-glutamine, and penicillin-streptomycin at 37°C in an atmosphere of 5% CO_2 (18). HEK cells were maintained in Dulbecco's modified Eagle's medium/Ham's nutrient mixture F12 supplemented with 10% fetal calf serum, 100 U/ml penicillin, 100 μg/ml streptomycin, 100 mM HEPES, and 2 mM L-glutamine. Stably transfected cell lines expressing G501S and R499C were created using the same approaches previously employed to analyze normal and specific mutants of human MPO(17). PCR was used to mutate G501 or R499C in normal MPO cDNA for heterologous expression in human cell lines which are devoid of endogenous MPO. The forward and reverse primers for mutagenesis of G501 were GCCTTCCGCTAC**A**GCCACACCCTCA and TGAGGGTGTGGC**T**GTAGCGGAAGGC, respectively, with the mutated residue indicated in bold text, whereas primers ACCAATGCCTTC**T**GCTACGGCCACA and TGTGGCCGTAGC**A**GAAGGCATTGTT were used to create R499C. The presence of the desired mutation and absence of unintentional mutations were confirmed by sequencing the cDNA prior to transfection. Once the sequence of the desired mutant construct was confirmed, it was cloned into the expression vector [pREP10 for K562 cells and pcDNA3.1 (-) for HEK cells]. Stable transfectants were cloned by limiting dilution and selected using hygromycin and G-418 sulfate, respectively.

MPO biosynthesis by transfectants

Stably transfectants were used for the expression of wild-type and mutant forms of MPO (17;18;24;26). Cells were maintained at low density in media supplemented with 2 μg/ml hemin for 24 hours prior to labeling and placed in methionine-free RPMI supplemented with fetal calf serum and antibiotics for 1 hour prior to pulse labeling with [^{35}S]-methionine/cysteine. Cells were labeled for the indicated period and then recovered, or chased by the addition of 1000-fold excess of cold methionine, before solubilization for subsequent analysis.

MPO-related products were immunoprecipitated using antibodies against MPO, CRT, or CLN. Biosynthetically radiolabeled MPO-related proteins in cell lysates or culture medium were immunoprecipitated with monospecific, polyclonal rabbit anti-human MPO (27), (17;18;24;26;28-31)separated by SDS-PAGE followed by autoradiography, and quantitated by direct measurement of radioactivity using a phosphorimager (Typhoon 9410, Amersham Biosciences, Piscatawy, NJ).

MPO-related species that were associated with CRT or CLN were recovered and quantitated using sequential immunoprecipitations (17;24;26). Cell lysates were immunoprecipitated first with CRT or CLN antiserum under nondenaturing conditions. The CRT- or CLN-associated proteins in the recovered complex were released by heating in the presence of 2% SDS and the solution was cooled and diluted 10-fold before proceeding with the

immunoprecipitation with MPO antiserum. CRT- and CLN-associated MPO species were separated by SDS-PAGE and quantitated using the phosphorimager.

Heme acquisition was assessed by radiolabeling with [^{14}C]-δ-aminolevulinic acid, a precursor in heme synthesis, as done previously. Stable transfectants expressing normal or mutant MPO were cultured in the presence of [^{14}C]-δ-aminolevulinic acid overnight, followed by solubilization and immunoprecipitation of the cell lysate or conditioned culture media with MPO-antibody, as described above. [^{14}C]-containing MPO species were quantitated with the phosphorimager.

MPO activity

Four different assays were employed to assess MPO activity. Peroxidase activity of the expressed wild type or mutant MPO was quantitated in two complementary ways. Non-transfected cells, normal MPO transfectants, and transfectants expressing mutant MPO were cultured in the presence of 2 μg/ml hemin for 48 hours prior to recovery and solubilization for determination of enzymatic activity. Peroxidase activity was quantitated spectrophotometrically using *o*-dianisidine as a substrate (32). Peroxidase activity in cell lysates was also assessed by *in situ* staining in a native polyacrylamide gel. Duplicate samples were electrophoresed under non-denaturing conditions into two 10% polyacrylamide gels containing 0.05% (w/v) cetyltrimethylammonium bromide and 25% glycerol (w/v) in the absence of a stacking gel. Samples were electrophoresed at constant voltage (100 V) toward the cathode until the dye front was ~ 5 mm from the bottom of the gel (approximately 5 hours). To avoid permanently staining the Scotch brite pads with crystal violet, we often electrophorese the dye front off the gel (800-1000 V-hrs) when subsequently blotting native gels. One gel was washed and stained with trimethylbenzidine to assess peroxidase activity (33-35). The other gel was soaked in transfer buffer for 1 hour and then subjected to electroblotting to a nitrocellulose filter for 850 V-hours. The resulting blot was blocked and then processed with MPO-antiserum. By performing both analyses in parallel, peroxidase activity could be assigned to a specific protein immunochemically related to MPO.

The greater amounts of mutant protein generated by HEK transfectants made possible two additional assays that are specific for MPO. We quantitated the capacity of HEK cell lysates, either wild-type or transfectants expressing normal or mutant MPO, to consume H_2O_2, using a H_2O_2 electrode and modification of a previously described method (36). In the presence of chloride, H_2O_2 consumption by MPO reflects HOCl production. The electrode (Apollo 4000, World Precision Instruments, Sarasota, FL) was calibrated daily with dilutions of reagent grade H_2O_2 (0-20 mM), with the concentrations of the H_2O_2 standard verified spectrophotometrically using ε_{240} = 43.6 $M^{-1}cm^{-1}$ (37). Cell lysates were added to known amounts of H_2O_2 in the presence of taurine, to scavenge HOCl and thus eliminate the possibility of its inactivation of the MPO (36), and the rate of H_2O_2 consumption measured polarigraphically. Data are expressed as nmoles H_2O_2 consumed per min per cell equivalent.

The lysates were likewise assessed for MPO-specific chlorinating capacity using the taurine chloramine assay (36). HOCl reacts with taurine to generate taurine monochloramine with in turns reacts with 5-thio-2-nitrobenzoic acid to generate 5,5'-dithiobis(2-nitrobenzoic acid). The concentration of taurine monochloramine measured spectrophotometrically, ε_{412} = 14.1 $M^{-1}cm^{-1}$, and its loss were monitored as a reflection of HOCl production. Lysates from wild-type or transfected cells were used as the potential peroxidase source and acetaldehyde-xanthine oxidase served as a source for generating oxidants. Data are expressed as nmoles of HOCl produced/min. All assays were performed in triplicate and each experiment was performed at least three times. We confirmed our findings in a more sensitive and specific assay for MPO-dependent chloramine production which uses iodide-dependent oxidation of 3.3'5.5'-tetramethylbenzidine as substrate (38). As

little as 200 pM MPO can be detected using this assay.

Glycosidase susceptibility of MPO-related proteins

Modifications of the carbohydrate sidechains on MPO-related proteins were assessed by their relative susceptibility to endoglycosidases as done previously with MPO endogenously expressed in myeloid precursors (31;39). MPO-related proteins were immunoprecipitated from cell lysates or culture medium at specified time points and treated with endoglycosidase H or N-glycanase to digest high mannose or complex carbohydrate sidechains, respectively. Digested proteins and control immunoprecipitates were separated by SDS-PAGE and visualized by autoradiography.

Spectroscopy

Just as the endogenous MPO synthesized by myeloid precursors is largely compartmentalized into an intracellular organelle (1), MPO expressed by HEK cells was stored in membrane-bound organelles that could be recovered by differential centrifugation. HEK cells (1-2.5 x 10^8) were collected, treated with diisopropylfluorophosphate, washed and resuspended in relaxation buffer (10 mM PIPES, 100 mM KCl, 3 mM NaCl, 3.5 mM $MgCl_2$, 1 mM ATP, pH 7.3) at 2 x 10^7/ml. Cells were then disrupted by N_2 cavitation (350 psi) and the cavitate was collected in a volume of EGTA, pH 7.4, to achieve a final concentration of 1.25 mM, using a method previously employed for recovering intact intracellular organelles from human neutrophils (40) and cultured promyelocytic cell lines (32). Unbroken cells and nuclei were removed by low speed centrifugation and the supernatant centrifuged at 12,000g x 20 min (4°C) to recover a pellet enriched for dense intracellular organelles, including those containing MPO-related proteins. The pellet was resuspended in PBS without calcium or magnesium, washed, and lysed by three freeze-thaw cycles using vigorous pipetting. Vigorous pipetting at each step is essential to maximize vesicle disruption. The clarified supernatant after pellet lysis was scanned from 400 to 600 nm in a Lambda 40 spectrophotometer (Perkin Elmer, Wellesley, MA). In addition, oxidation-reduction difference spectroscopy was performed, using dithionite to reduce the lysate in the sample cuvette. The concentration of normal MPO was calculated for oxidized samples using ε_{430} = 91 $mM^{-1}cm^{-1}$ (41). For turbid samples reduced minus oxidized difference spectra were obtained and concentration calculated using ε_{473} = 75 $mM^{-1}cm\text{-}^{1}$(41). For assays using mutant MPO, the same extinction coefficients were employed to approximate the concentrations of G501S and R499C.

RESULTS

Identification of MPO deficient subjects

As part of ongoing studies of the prevalence of inherited MPO deficiency in Japan (42), individuals with partial or complete deficiency were identified using automated flow hematocytochemistry to screen large populations. Among these deficient individuals were two with missense mutations in MPO, G501S and R499C, that had not been previously reported. In both cases, the individuals were asymptomatic and had not suffered from frequent or severe infectious complications, as described in the detailed clinical reports (21;22;42).

Predictions derived from molecular modeling.

Given the availability of the crystal structure of human MPO (11), we modeled the heme pocket of specific mutants at residues 499 and 501 for comparison with the native protein and to gain insights into their potential impact on MPO enzymatic activity. The iron ion in native MPO has six coordination sites: four sites are mediated by pyrrole nitrogen atoms in the heme, whereas the fifth coordination is the axial H502-Fe bond. The sixth coordination site on the iron ion is vacant and serves to accept electrons and thereby participate in the electrochemistry of the iron-catalyzed oxidation (43) (Figure 1A).

The heme in MPO is covalently bound to the protein through two ester linkages and a methionyl sulfonium linkage (11). In addition to the three covalent bonds, electrostatic

interactions with pyrrole rings C and D contribute to the structure and stability of the heme pocket in MPO. The guanidinium group of R499, as well as that of R590, forms hydrogen bonds with the carboxyl group of a propionate in ring D (11). Replacement of R499 with any residue that eliminates this electrostatic interaction would likely compromise heme binding and stability. Furthermore, after arranging the side-chains in R499C to optimize favorable interactions with the molecular neighbors, the model of the heme pocket predicted sufficient space and side-chain mobility to afford close proximity between its sulfur atom and the heme iron, were heme incorporated into the pocket lacking the stabilizing arginine at 499. Whether in a neutral or deprotonated state, the sulfur introduced by R499C could coordinate with the iron, thereby forming a relatively strong interaction at ~ 2.5 Å (Figure 1B). Such strong polar or covalent interaction could significantly compromise redox properties of the iron ion and thereby compromise the enzymatic activity of the mutant protein. Thus, the model predicts two consequences from R499C, one reflecting the loss of an important stabilizing electrostatic interaction with arginine and the other the introduction of a disruptive cysteine.

The optimized model of G501S likewise demonstrated potential changes that could compromise the function of the heme (Figure 1C). The replacement of glycine with serine may leave inadequate space to stably accommodate the heme group. Furthermore, if the substitution was tolerated, replacement of glycine with serine would reduce the flexibility of the protein backbone in the heme environs might be reduced. Whereas the highly flexible G501 in native MPO allows close approximation of the aromatic nitrogen in H502 below the heme iron atom, the loss of flexibility after the serine replacement might disturb proper heme function. Taken together, the simplistic models of each of the naturally occurring mutations in such close proximity to the redox center of MPO predicted structural consequences likely to compromise optimal function of the heme group.

Failure of G501S precursor to undergo proteolytic maturation

To examine directly the impact of these missense mutations on the fate of the protein, we created stable transfectants and compared synthesis of the mutant proteins with that of normal MPO. Stably transfected K562 cells expressing normal or G501S MPO were radiolabeled for 1 hour and chased for 0 or 20 hours before recovery of cells and the conditioned medium for immunoprecipitation. K562 transfectants expressing either normal or G501S MPO synthesized a 90-kDa protein after 1 hour of labeling (Figure 2). In the case of normal MPO, the 90-kDa protein underwent proteolytic processing during the 20 hours of chase to yield the 59-kDa and 13.5-kDa subunits of mature MPO. However, the precursor in G501S cells failed to yield the 59-kDa heavy subunit and more 90-kDa precursor was present during the chase period in G501S-expressing cell than in transfectants expressing normal MPO, indicating that the absence of mature MPO reflected failure to undergo processing into MPO subunits and not rapid degradation of the mutant G501S precursor.

Normal and G501S-expressing cells secreted the same amounts of 90-kDa MPO protein into the culture medium during the chase period (Figure 2), suggesting that normal amounts of the G501S precursor entered the secretory pathway despite the failure of proteolytic maturation to proceed. As previously reported for normal MPO biosynthesis (20), approximately 10% of MPO precursor is secreted constitutively and undergoes limited modification of its oligosaccharide sidechains during transit through the Golgi, whereby the secreted species is partially resistant to endoglycosidase H digestion (39). To determine if the secreted MPO precursor from transfectants expressing G501S underwent oligosaccharide modification, the lysates of pulse-labelled cells and supernatants conditioned by the 20 hour chase period were recovered from each cell line, immunoprecipitated with MPO antiserum, and subjected to digestion with endoglycosidase H or N-glycanase to cleave high mannose or

both high mannose and complex mannose sidechains, respectively. The oligosaccharides on the intracellular 90-kDa MPO precursors of normal and G501S were both fully susceptible to digestion with endoglycosidase H, indicating that the sidechains were exclusively high-mannose in nature (Figure 3). However, the carbohydrates on the secreted MPO precursor were partially endoglycosidase H-resistant, evidenced by limited digestion with endoglycosidase H but complete removal by N-glycanase treatment. The G501S mutant behaved in a fashion identical to that of normal MPO, suggesting that the G501S precursor entered the constitutive secretory pathway and was modified by Golgi resident enzymes in a normal fashion.

During normal biosynthesis MPO precursors interact transiently with calreticulin (CRT), calnexin (CLN), and ERp57 (20), all molecular chaperones in the ER that contribute to the proper folding of many glycoproteins (44). Pulse-labelled K562 cells transfected with normal or G501S MPO were chased for 0, 1, 2, or 4 hours and the lysates immunoprecipitated in parallel with antibodies against MPO, CRT, or CLN under nondenaturing conditions, as previously described. To recover the CRT- and CLN-associated MPO precursor at each time point, the immunoprecipitates were denatured and subjected to a second immunoprecipitation using the MPO antibody (Figure 4). In both transfectants expressing normal and G501S MPO, the recoveries of CRT-associated and CLN-associated MPO precursor were the same as previously reported for normal MPO (24;26), suggesting that the interactions between CRT or CLN with MPO precursors were not significantly altered by the G501S missense mutation.

Activity of G501S precursors expressed in K562 cells

Normal MPO biosynthesis requires the insertion of heme into apoproMPO in the ER, thereby converting an enzymatically inactive 90-kDa MPO precursor into a 90-kDa protein with peroxidase activity (45). We assessed first the peroxidase activity of the G501S product spectroscopically using *o*-dianisidine as the substrate. K562 cells lack endogenous MPO (18) and exhibited very low background peroxidase activity in this assay (0.9 IU). In contrast, an identical number of PLB-985 cells, a human promyelocytic cell line that actively synthesizes structurally and functionally normal MPO (24), had 17.2 IU of peroxidase activity. K562 cells transfected with normal MPO had 4.9 IU of peroxidase activity (n=5), whereas G501S transfectants had 0.5 IU of activity, levels indistinguishable from baseline. Because we were concerned that the relatively low efficiency of MPO expression in the K562 cell system might undermine our capacity to detect very low levels of activity by the G501S, we examined the suitability of using HEK cells for biosynthetic studies, based on its successful application to generating recombinant protein for use in immunological characterization of anti-MPO mediated vasculitis (46).

MPO biosynthesis by HEK transfectants

Wild-type HEK cells lack endogenous MPO but after transfection synthesized heme-containing precursors that underwent normal proteolytic processing to mature MPO and efficient targeting to an intracellular, membrane-bound compartment that could be pelleted by centrifugation (Figure 5). All aspects of MPO biosynthesis seen in cultured myeloid cells were reproduced in the HEK-MPO system. Specifically, the 90-kDa apoproMPO acquired heme in the ER to form proMPO and precursors interacted with molecular chaperones ERp57, CRT, and CLN (Figure 6) with the same selectivity previously reported for the K562 transfectants (24;26). Heme acquisition was necessary for exit from the ER and for proteolytic processing to mature subunits, with the latter event inhibited by disruption of the Golgi by treatment with brefeldin A (data not shown). Approximately 10% of MPO precursor entered the secretory pathway and underwent limited modification of its oligosaccharide sidechains, as seen with MPO endogenously produced by cultured promyelocytes (39). The spectral properties of MPO-enriched pellets recovered from stable transfectants were identical to those of normal MPO (see below), with a λ_{max} of 430 nm for

the oxidized sample and a Soret band at 473 nm for the reduced minus oxidized spectroscopy (41). Taken together, the data indicate that the HEK transfectants faithfully mirrored the events in normal MPO biosynthesis previously identified in myeloid precursors.

Most important for our studies was the improved level of MPO expression in HEK cells relative to that in the K562 transfectants. Wild-type HEK cells lack any evidence of endogenous MPO, as judged immunochemically, spectroscopically, or by assessing enzymatic activity. In contrast, the specific activity of HEK-MPO (4.2 nmoles H_2O_2 consumed/min/pmoles MPO, n=3) was the same as partially purified MPO recovered from granules of normal PMN (3.3 nmoles H_2O_2 consumed/min/pmoles MPO, n=3) or the human promyelocytic cell line PLB-985 cultured in hemin (3.6 nmoles H_2O_2 consumed/min/pmoles MPO, n=3) . Although the amount of MPO in transfectants (3.9 pmoles MPO/10^6 cells, n=3) was lower than that in normal PMN (11.7 pmoles MPO/10^6 cells, n=3) or in PLB-985 cells grown in the presence of hemin (11pmoles MPO/10^6 cells, n=3), HEK transfectants provided a system to yield levels of protein sufficient to perform spectroscopy and reliably assess function of specific mutants.

HEK-R499C, a second mutation near the critical proximal histidine in the heme pocket

To assess the impact of the R499C missense mutation on MPO biosynthesis both in relation to normal MPO and to G501S, we created stably transfected HEK cell lines expressing the mutant forms of MPO. After one hour of biosynthetic labeling with [^{35}S]-methionine, HEK-R499C associated with CRT, CLN, and ERp57 to the same extent as did wild-type MPO (Figure 6) and the rates of dissociation during the chase were likewise the same (data not shown**)**. Both R499C and G501S lacked enzymatic activity in native activity gels (Figure 7). The HEK-R499C resembled G501S with respect to proteolytic processing, as both mutations resulted in synthesis of a 90-kDa species that was secreted normally but was not processed into mature subunits after a 20 hour chase (Figure 8A). As both mutants were enzymatically inactive and failed to undergo normal maturation, we anticipated that neither incorporated heme. However transfectants expressing normal or mutant MPO and labeled with [^{14}C]-δ aminolevulinic acid, a precursor of heme, synthesized the 90-kDa proMPO that was released into the culture medium (Figure 8B). When normalized for the [^{35}S]-methionine content in MPO precursors, heme incorporation was 28.7 ± 2.9% and 23.7 ± 1.6% of control for R499C and G501S, respectively (n=3). Based on these data and the amount of heme in HEK-MPO cells (3.9 pmoles/10^6 cells), we estimate that R499C and G501S transfectants contained ~1.12 and 0.92 pmoles of heme-containing MPO-related protein per 10^6 cells. Thus, in both mutants there was a maturation arrest at the stage of heme incorporation, whereby heme acquisition by mutant apoproMPO was inefficient or the mutant proMPO was unstable and rapidly degraded. The stability of the mutant precursors was not increased by culturing cells in the presence of proteasome inhibitors (data not shown), in contrast to the proteasome-mediated degradation seen with the MPO mutant Y173C (17), indicating that if degradation of mutant proteins occurred, it was not mediated by the proteasome.

Given the failure of either mutant to exhibit peroxidase activity *in vitro*, we anticipated that neither would chlorinate taurine. Neither G501S nor R499C chlorinated taurine (data not shown) and the capacity for G501S or R499C to consume H_2O_2 was low, 0.52 and 0.65 nmoles/min/cell equivalent respectively, and no different from that of wild-type HEK cells (0.91 nmoles/min/cell equivalent). In contrast, HEK transfectants expressing normal MPO were fully active (5.75 nmoles/min/cell equivalent), suggesting that although the mutant had incorporated heme, the resultant proMPO was not competent to mediate peroxidative events. To compare the spectral properties of normal and mutant proteins, samples enriched for the intracellular compartment in HEK cells containing normal and mutant MPO were

prepared. The presence of MPO-related proteins in each pellet was confirmed by immunoblotting (data not shown). Although all four samples had identical spectra in the 200-400 nm range (data not shown), significant differences were noted in the Soret absorbance region. Wild-type HEK cells lacked a Soret peak between 400 and 500 nm (Figure 9), whereas the pellets recovered from normal PMN or from HEK transfectants expressing normal MPO exhibited a peak at 430 nm, characteristic of MPO (41). In contrast, pellets from HEK transfectants expressing R499C or G501S exhibited a Soret band at 414 nm, with no detectable signal at 430 nm. The observed red-shift of the absorbance peak in the mutant proteins suggests that each of the alterations near histidine 502, critical for binding on the proximal side of the heme, altered the structural conformation of the heme.

DISCUSSION

Mature MPO normally resides exclusively in the azurophilic granules of PMN and monocytes, compartments containing a variety of hydrolytic enzymes [see (1) for review of MPO biology]. Concomitant activation of the NADPH-dependent oxidase, a source of reactive oxygen species including H_2O_2, and release of granule contents, including MPO, into the newly formed phagolysosome, deliver to the ingested microorganism a variety of toxic reactants that synergistically mediate efficient killing [reviewed in (3)]. Among these noxious agents is HOCl, the result of the unique property of MPO to catalyze the 2-electron peroxidation of Cl^- in the presence of H_2O_2(47). HOCl is extremely toxic to bacteria; 10^8 HOCl molecules/cell can kill 5 g of *E.coli*, whereas > 10^{11} molecules of H_2O_2 (under metal-free conditions) or hydroxyl radical are necessary to achieve the same cytotoxicity (48-50). Several lines of evidence support the importance of the MPO-H_2O_2-Cl^- system in oxygen-dependent microbicidal activity against a wide spectrum of organisms, including viruses, bacteria, fungi, protozoa, and tumor cells as well as promoting inflammation *per se* [reviewed in (47)]. Given that MPO and its unique chemistry appear especially well suited for a central role in antimicrobial activity, elucidation of critical structural determinants is essential to understand the basis for its biological action.

Heme peroxidases can be categorized into three superfamilies based on sequence: catalases, plant peroxidases, and mammalian peroxidases (51). Mammalian peroxidases include the cyclooxygenase and myeloperoxidase families, the later composed of MPO, eosinophil peroxidase (EPO), lactoperoxidase (LPO), and thyroid peroxidase (TPO)(52;53). These peroxidases share the unique property of having two or three covalent bonds between the heme and the mature enzyme. Availability of an expression system for MPO biosynthesis and processing that faithfully mirrors the endogenous events in myeloid cells is an analytical tool necessary for the study of structure-function relationships in the heme pocket of animal peroxidases. Previous studies of the structural features of the heme environment of MPO that employed mutagenesis [reviewed in (54)] relied on recombinant protein isolated from transfectants unable to synthesize the functional, normal subunits of MPO. The recombinant MPO produced in Chinese hamster ovary (CHO) cells used for these studies has oligosaccharide sidechains significantly different from native MPO, fails to undergo proteolytic processing into mature subunits, and is expressed only in the monomeric form (55). Such differences may have functional consequences. For example, mutation of M409 to the corresponding residue in EPO (T), TPO (V), or LPO (Q) altered the spectral properties of the recombinant protein and eliminated its peroxidase activity (56), an unexpected finding given that this replacement normally exists in these related peroxidases. Given the quality control operative in the ER during MPO biosynthesis (17;57;58), it is possible that the observed deviations from normal biosynthesis have structural consequences that may undermine the interpretation of studies using the CHO-derived recombinant protein.

Although K562 transfectants expressing normal MPO recapitulate biosynthetic events seen in myeloid cells

expressing endogenous MPO, the yields of recombinant protein are insufficient for structural or functional studies. As an essential component of this study, we established that HEK cells stably transfected with normal MPO exhibited seminal features of the biosynthesis and proteolytic processing of MPO as first characterized in myeloid precursors [reviewed in (17)](18;24;26;28;30;31;57;59-63). The primary translation product in HEK cells underwent cotranslational cleavage of the signal peptide, N-linked glycosylation, and limited deglucosylation of high mannose oligosaccharide sidechains to generate the 90-kDa, enzymatically inactive precursor apoproMPO that interacted in the ER transiently and reversibly with the molecular chaperones ERp57, CRT, and CLN with subsequent incorporation of heme to generate the enzymatically active 90-kDa proMPO. Heme synthesis inhibition blocked proteolytic maturation as well as export of MPO precursor from the ER, indicating that its acquisition of heme induced conformational changes necessary for successful maturation and intracellular targeting. Although 10% of proMPO entered the secretory pathway and was recovered from the culture media, as reported for myeloid cells (64;65), most proMPO underwent modification of oligosaccharide sidechains and proteolytic processing *en route* to a membrane-bound intracellular compartment. We believe that our expression system provides sufficient material that mirrors the native protein and is thus especially well suited to address several specific questions of structure-function relationships raised by its crystal structure.

Among the animal peroxidases, only MPO has been crystallized, with structures of both the human and canine enzyme published. Based on the crystal structure of human MPO at 1.8 Å (11), the heme pocket is in a crevice ~ 15-20 Å deep and is solvent accessible via an open channel at the catalytic site on the distal side of the heme (53). There is significant amino acid identity among the animal peroxidases in the four helices that surround the heme group and several lines of evidence(4;66-68) implicate five residues in binding heme in MPO. Histidines at residues 261 and at 502 represent the distal and proximal ligands, respectively, and heme is covalently bound to MPO at three sites: through a methionyl sulfonium linkage with M409 and through ester linkages to E408 and D260 (11;69). The heme-protein interaction is further stabilized by hydrogen bonding between the carbonyl groups of ring C and D propionates and T266, D264, R499, R590, and water molecules (11). Although crystal structures for other family members have not been solved, modeling of homologous domains, NMR, mass spectrometry, and peptide analysis support the presence of the same two ester linkages in LPO, EPO, and TPO (11;70-74). Ester bonds account for the 10 nm shift in the Soret band of LPO, EPO, and TPO relative to horseradish peroxidase and the presence of the third covalent bond in MPO causes the red-shift of the Soret band of oxidized MPO (λ_{max} = 430 nm) relative to the spectral peak for the other family members [λ_{max} = 412 nm] (73;75;76). The peculiar sulfonium linkage in MPO likely contributes as well to its unique facility to oxidize Cl^- to HOCl at physiologic pH. The presence of covalent bonds between the prosthetic group and the protein is a feature unique to the animal peroxidases (51) and a H_2O_2-dependent autocatalytic process has been implicated in ester bond formation (72), although the precise mechanisms of ester bond formation in animal peroxidases and of sulfonium linkage in MPO *in vivo* are unknown. Although at least one covalent bond is required for peroxidase activity and the presence of covalent bonds with heme is a feature shared by all animal peroxidases, the functional or biological advantage of covalently bound heme is not known (73). Recent studies indicate that the presence of a single covalent bond between the heme group and its protein is sufficient to protect the heme vinyl group from modification by hypohalous acid generated by peroxidases (77-79). In this way, peroxidases such as MPO can generate large amounts of HOCl and its byproducts within the neutrophil phagosome without incurring autoinactivation by modification of the heme vinyl groups and subsequent inactivation.

In this manuscript we describe the impact of two novel mutations on the biosynthesis and function of human MPO. The target residues, G501 and R499, are present on the proximal side of the heme pocket and are conserved in all four members of the animal peroxidase family. Whereas both missense mutations compromised proper proteolytic processing and intracellular targeting of mature MPO, the precursors for each incorporated heme, albeit inefficiently. Both biosynthetic radiolabeling of heme (Figure 8) and spectroscopy (Figure 9) demonstrated the presence of small amounts of heme in the proproteins of G501S and R499C. However, the Soret band was blue-shifted in each, demonstrating a spectrum more akin to that seen with LPO, TPO, or EPO rather than that characteristic of native MPO. Although the spectra of the mutants were consistent with the presence of heme covalently bound, likely via two rather than three bonds, neither had enzymatic activity. Given the known electrostatic interaction between R499 and the ring D propionates of the heme in MPO, we predicted that the loss of this critical arginine would itself compromise heme binding and stability. Furthermore, the presence of cysteine at this site might allow a strong polar or covalent interaction between the sulfur atom in C499 and the heme iron, which could reduce the oxidation potential and enzymatic activity of the mutant MPO. In the case of changes at codon 501, glycine may be the only amino acid at that site that allows optimal heme binding, consistent with our spectral data indicating incorporation of only small amounts of heme. For any serine that is incorporated in the heme pocket, our modeling of G501S suggested that its dysfunction reflects the increased distance between the heme iron and its distal histidine at 502, which is predicted to be twice that present in normal MPO, consistent with the loss of one coordination site for the heme iron, as suggested experimentally by the spectroscopy.

Taken together, these studies of biosynthesis and biochemical characterization of mutant MPO expressed in HEK cells demonstrated the structural and functional impact of two naturally occurring missense mutations underlying hereditary myeloperoxidase deficiency. Future applications of these analytical techniques to other mutations, both experimentally created and spontaneously occurring, should provide novel insights regarding the structure-function relationships unique to the animal peroxidase protein family.

REFERENCES

1. Klebanoff, S. J. (2005) *J.Leuk.Biol.* **77,** 598-625
2. Nauseef, W. M. (2004) *Histochem.Cell Biol.* **122,** 277-291
3. Hampton, M. B., Kettle, A. J., and Winterbourn, C. C. (1998) *Blood* **92,** 3007-3017
4. Hazen, S. L., Hsu, F. F., Mueller, D. M., Crowley, J. R., and Heinecke, J. W. (1996) *J.Clin.Invest.* **98,** 1283-1289
5. Hazen, S. L., Hsu, F. F., and Heinecke, J. W. (1996) *J.Biol.Chem.* **271,** 1861-1867
6. Henderson, J. P., Byun, J., and Heinecke, J. W. (1999) *J.Biol.Chem.* **274,** 33440-33448
7. Hazen, S. L., d'Avignon, A., Anderson, M. M., Hsu, F. F., and Heinecke, J. W. (1998) *J.Biol.Chem.* **273,** 4997-5005
8. Hazen, S. L., Hsu, F. F., d'Avignon, A., and Heinecke, J. W. (1998) *Biochemistry* **37,** 6864-6873
9. Domigan, N. M., Charlton, T. S., Duncan, M. W., Winterbourn, C. C., and Kettle, A. J. (1995) *J.Biol.Chem.* **270,** 16542-16548
10. Winterbourn, C. C., Pichorner, H., and Kettle, A. J. (1997) *Arch.Biochem.Biophys.* **338,** 15-21
11. Fiedler, T. J., Davey, C. A., and Fenna, R. E. (2000) *J.Biol.Chem.* **275,** 11964-11971
12. Furtmüller, P. G., Zederbauer, M., Jantschko, W., Helm, J., Bogner, M., Jakopitsch, C., and Obinger, C. (2006) *Arch.Biochem.Biophys.* **445,** 199-213
13. Furtmüller, P. G., Burner, U., and Obinger, C. (1998) *Biochemistry* **37,** 17923-17930
14. Marquez, L. A. and Dunford, H. B. (1994) *J.Biol.Chem.* **269,** 7950-7956
15. Furtmüller, P. G., Obinger, C., Hsuanyu, Y., and Dunford, H. B. (2000) *Eur.J.Biochem.* **267,** 5858-5864
16. Marchetti, C., Patriarca, P., Solero, G. P., Baralle, F. E., and Romano, M. (2004) *Hum.Mutation* **23,** 496-505
17. DeLeo, F. R., Goedken, M., McCormick, S. J., and Nauseef, W. M. (1998) *J.Clin.Invest.* **101,** 2900-2909
18. Nauseef, W. M., Cogley, M., and McCormick, S. (1996) *J.Biol.Chem.* **271,** 9546-9549
19. Nauseef, W. M., McCormick, S., and Goedken, M. (2000) *Redox Report* **5,** 197-206
20. Hansson, M., Olsson, I., and Nauseef, W. M. (2006) *Arch.Biochem.Biophys.* **445,** 214-224
21. Ohashi, Y. Y., Kameoka, Y., Persad, A. S., Koi, F., Yamagoe, S., Hashimoto, K., and Suzuki, K. (2004) *Gene* **327,** 195-200
22. Persad, A. S., Kameoka, Y., Kanda, S., Niho, Y., and Suzuki, K. (2006) *Gene Expression* **13,** 1-5

23. Nauseef, W. M., Root, R. K., and Malech, H. L. (1983) *J.Clin.Invest.* **71,** 1297-1307

24. Nauseef, W. M., McCormick, S. J., and Clark, R. A. (1995) *J.Biol.Chem.* **270,** 4741-4747

25. MacKerell, A. D., Bashford, D., Bellott, M., Dunbrack Jr, R. L., Evanseck, J. D., Field, M. J., Fischer, S., Gao, J., Guo, H., Ha, S., Joseph-McCarthy, D., Kuchnir, L., Kuczera, K., Lau, F. T. K., Mattos, C., Michnick, S., Ngo, T., Nguyen, D. T., Prodhom, B., Reiher III, W. E., Roux, B., Schlenkrich, M., Smith, J. C., Stote, R., Straub, J., Watanabe, M., Wiórkiewicz-Kuczera, J., Yin, D., and Karplus, M. (1998) *J.Phys.Chem.B* **102,** 3586-3616

26. Nauseef, W. M., McCormick, S. J., and Goedken, M. (1998) *J.Biol.Chem.* **273,** 7107-7111

27. Bülow, E., Nauseef, W. M., Goedken, M., McCormick, S., Calafat, J., Gullberg, U., and Olsson, I. (2002) *J.Leukoc.Biol.* **71,** 279-288

28. Nauseef, W. M., McCormick, S., and Yi, H. (1992) *Blood* **80,** 2622-2633

29. Nauseef, W. M., Olsson, I., and Strömberg-Arnljots, K. (1988) *Eur.J.Haematol.* **40,** 97-110

30. Nauseef, W. M. (1986) *Blood* **67,** 865-872

31. Nauseef, W. M. (1987) *Blood* **70,** 1143-1150

32. Nauseef, W. M. and Clark, R. A. (1986) *Blood* **68,** 442-449

33. Olsen, R. L. and Little, C. (1983) *Biochem.J.* **209,** 781-787

34. Pember, S. O., Shapira, R., and Kindade, J. M., Jr. (1983) *Arch.Biochem.Biophys.* **221,** 391-403

35. Van Dalen, C. J., Whitehouse, M. W., Winterbourn, C. C., and Kettle, A. J. (1997) *Biochem.J.* **327,** 487-492

36. Kettle, A. J. and Winterbourn, C. C. (1994) *Methods Enzymol.* **233,** 502-512

37. Beers, R. J. and Sizer, I. W. (1952) *J.Biol.Chem.* **195,** 133-140

38. Dypbukt, J. M., Bishop, C., Brooks, W. M., Thong, B., Eriksson, H., and Kettle, A. J. (2005) *Free Radic.Biol.Med.* **39,** 1468-1477

39. Andersson, E., Hellman, L., Gullberg, U., and Olsson, I. (1998) *J.Biol.Chem.* **273,** 4747-4753

40. Borregaard, N., Heiple, J. M., Simons, E. R., and Clark, R. A. (1983) *J.Cell Biol.* **97,** 52-61

41. Bos, A. J., Wever, R., and Roos, D. (1978) *Biochim.Biophys.Acta* **525,** 37-44

42. Kameoka, Y., Persad, A. S., and Suzuki, K. (2004) *Jpn J Infect Dis* **57,** S12-S13

43. Battistuzzi, G., Bellei, M., Zederbauer, M., Furtmüller, P. G., Sola, M., and Obinger, C. (2006) *Biochemistry* **45,** 12750-12755

44. Helenius, A., Trombetta, E. S., Hebert, D. N., and Simons, J. F. (1997) *Trends Cell Biol.* **7,** 193-200

45. Arnljots, K. and Olsson, I. (1987) *J.Biol.Chem.* **262,** 10430-10434

46. Erdbrügger, U., Hellmark, T., Bunch, D. O., Alcorta, D. A., Jennette, J. C., Falk, R. J., and Nachman, P. H. (2006) *Kidney Int.* **69,** 1799-1805

47. Klebanoff, S. J. (1999) *Proc.Assoc.Am.Physicians* **111,** 383-389

48. Elzanowska, H., Wolcott, R. G., Hannum, D. M., and Hurst, J. K. (1995) *Free Radic.Biol.Med.* **18,** 437-449

49. Wolcott, R. G., Franks, B. S., Hannum, D. M., and Hurst, J. K. (1994) *J.Biol.Chem.* **269,** 9721-9728

50. Hurst, J. K. and Lymar, S. V. (1999) *Acc.Chem.Res.* **32,** 520-528

51. Dunford, H. B. (1999) *Heme Peroxidases*, First Ed., Wiley-VCH, New York

52. Kimura, S. and Ikeda-Saito, M. (1988) *Proteins* **3,** 113-120

53. Zeng, J. and Fenna, R. E. (1992) *J.Mol.Biol.* **226,** 185-207

54. Moguilevsky, N. (2000) Structural and biological properties of human recombinant myeloperoxidase. In Nauseef, W. M. and Petrides, P. E., editors. *The peroxidase multigene family of enzymes*, Springer-Verlag,

55. Moguilevsky, N., Garcia-Quintana, L., Jacquet, A., Tournay, C., Fabry, L., Piérard, L., and Bollen, A. (1991) *Eur.J.Biochem.* **197,** 605-614

56. Kooter, I. M., Moguilevsky, N., Bollen, A., van der Veen, L. A., Otto, C., Dekker, H. L., and Wever, R. (1999) *J.Biol.Chem.* **274,** 26794-26802

57. Nauseef, W. M. (1999) *J.Lab.Clin.Med.* **134,** 215-221

58. Nauseef, W. M. (2003) Roles of calreticulin and calnexin in myeloperoxidase biosynthesis. In Eggleton, P. and Michalak, M., editors. *Calreticulin*, Landes Bioscience, Georgetown, Texas

59. Johnson, K. R., Nauseef, W. M., Care, A., Wheelock, M. J., Shane, S., Hudson, S., Koeffler, H. P., Selsted, M., Miller, C., and Rovera, G. (1987) *Nucleic Acids Res.* **15,** 2013-2028

60. Nauseef, W. M. (1989) *Blood* **73,** 290-295

61. Nauseef, W. M., Brigham, S., and Cogley, M. (1994) *J.Biol.Chem.* **269,** 1212-1216

62. Nauseef, W. M. (1998) *J.Mol.Med.* **76,** 661-668

63. Nauseef, W. M. (1988) Myeloperoxidase deficiency. In Curnutte, J. T., editor. *Hematology/Oncology Clinics of North America*, W.B. Sanders, Philadelphia

64. Yamada, M., Hur, S.-J., and Toda, H. (1990) *Biochem.Biophys.Res.Commun.* **166,** 852-859

65. Yamada, M., Mori, M., and Sugimura, T. (1981) *Biochemistry* **20,** 766-771

66. Kettle, A. J. and Winterbourn, C. C. (1990) *Biochim.Biophys.Acta Mol.Cell Res.* **1052,** 379-385

67. Zgliczynski, J. M., Stelmaszynska, T., Domanski, J., and Ostrowski, W. (1971) *Biochem.Biophys.Acta* **235,** 419-424

68. Strauss, R. R., Paul, B. B., Jacobs, A. A., and Sbarra, A. J. (1971) *Infect.Immun.* **3,** 595-602

69. Henderson, L. M. and Chappell, J. B. (1996) *Biochim.Biophys.Acta Bio-Energetics* **1273,** 87-107

70. DeGioia, L., Ghibaudi, E. M., Laurenti, E., Salmona, M., and Ferrari, R. P. (1996) *JBIC* **1,** 476-485

71. Ferrari, R. P. (2000) Structure function relationships amongst members of the animal peroxidase family of proteins. In Petrides, P. E. and Nauseef, W. M., editors. *The peroxidase multigene family of enzymes:biochemical basis and clinical applications*, Springer-Verlag, Berlin

72. DePillis, G. D., Ozaki, S., Kuo, J. M., Maltby, D. A., and Ortiz de Montellano, P. R. (1997) *J.Biol.Chem.* **272,** 8857-8860

73. Colas, C. and Ortiz de Montellano, P. R. (2003) *Chem.Rev.* **103,** 2305-2332

74. Fayadat, L., Niccoli-Sire, P., Lanet, J., and Franc, J.-L. (1999) *J.Biol.Chem.* **274,** 10533-10538

75. Kooter, I. M., Moguilevsky, N., Bollen, A., Sijtsema, N. M., Otto, C., and Wever, R. (1997) *J.Biol.Inorg.Chem.* **2,** 191-197

76. Brogioni, S., Feis, A., Marzocchi, M. P., Zederbauer, M., Furtmüller, P. G., Obinger, C., and Smulevich, G. (2006) *J.Raman Spectroscopy* **37,** 263-276

77. Huang, L., Wojciechowski, G., and Ortiz de Montellano, P. R. (2006) *J.Biol.Chem.* **281,** 18983-18988

78. Huang, L., Wojciechowski, G., and Ortiz de Montellano, P. R. (2005) *J.Am.Chem.Soc.* **127,** 5345-5353

79. Huang, L. and de Montellano, P. R. O. (2006) *Arch.Biochem.Biophys.* **446,** 77-83

FOOTNOTES:

[1] Because considerations of MPO include the propeptide, our amino acid designations are 166 greater (for the 166 amino acids in the propeptide) than those used by Fenna (11;53).

Acknowledgements: We thank Dr. Ramaswamy Subramanian for advice on mutational analysis. The work was supported by a HL 53592 and a Merit Review (Veterans Administration) to WMN.

FIGURE LEGENDS

Figure 1. **Models of the heme pockets of normal and mutant MPO**
(A) The proximal heme-binding residue, H502, and heme iron are depicted in a CPK model. His502 anchors 6-coordinated Fe+3 ion of the heme from underneath position, leaving the sixth coordination site above the heme available to react with substrate.(B) Normal MPO is depicted in green, R499C in yellow, and bromide (representing the halide binding site) in orange. The proximity of the sulfur atom of the cysteine of R499C is sufficient to exert significant electrostatic effect on the heme iron. (C) Normal MPO is depicted in green, with G501S in gray. Due to steric limitations, the replacement of glycine with serine at residue 501 may significantly compromise heme binding. Furthermore, if possible, substitution of the flexible G501 residue with serine would compromise backbone flexibility (backbone 'hinge') in the heme pocket and consequently promote the departure of the H502 anchoring side chain from the iron ion.

Figure 2. **Biosynthesis of normal and G501S MPO by transfected K562 cells**
K562 cells stably transfected with wild-type MPO (WT) or G501S mutant MPO (G501S) were pulse-labelled with [^{35}S]-methionine and chased for 0 or 20 hours. Cell lysates at 0 and 20 hours and culture medium at 20 hrs were immunoprecipitated with anti-MPO. Immunoprecipitates were separated by SDS-PAGE and dried gels subjected to autoradiography. Cells expressing G501S synthesized and secreted a 90-kDa precursor form of MPO but failed to process it into the mature MPO, represented by the generation of the 59-kDa heavy subunit of the native protein.

Figure 3. **Glycosylation of normal and G501S MPO produced by K562 transfectants**
After 1 hour of biosynthetic pulse labeling with [^{35}S]-methionine and a 20 hour chase, cell lysates and culture medium from K562 cells expressing normal (WT) or mutant (G501S) MPO were immunoprecipitated with anti-MPO. Immunoprecipitates were incubated with buffer alone (C), endoglycosidase H (H), or N-glycanase (N) before recovery and analysis by SDS-PAGE and autoradiography. Fully glycosylated precursor migrated at 90-kDa, whereas the non-glycosylated product was 80-kDa. Arrows indicate individual glycosylated products. For both normal and mutant MPO, secreted MPO precursors were more resistant to endoglycosidase H digestion than were the intracellular forms.

Figure 4. **Association of molecular chaperones with normal and G501S MPO in K562 cells**
K562 transfectants expressing normal (wild-type) or G501S MPO were biosynthetically radiolabeled for 1 hour and chased with cold methionine for 0 to 4 hours. Cell lysates were immunoprecipitated with anti-MPO or sequentially with anti-CRT or anti-CLN followed by anti-MPO. Resulting immunoprecipitates were analyzed by SDS-PAGE and autoradiography. Like normal MPO, the G501S precursor associated transiently with CRT and CLN.

Figure 5. **Biosynthesis of normal MPO by stably transfected HEK cells stably**
Wild-type HEK cells (WT) or HEK cells stably expressing normal MPO (MPO) were biosynthetically radiolabeled, with intervals of chase of 0 and 20 hours. Cell lysates and culture medium were immunoprecipitated with anti-MPO and the immunoprecipitates analyzed by SDS-PAGE and autoradiography. Wild-type HEK cells lacked endogenous MPO. When expressed in HEK cells, MPO precursors were synthesized, secreted, and proteolytically processed intracellularly in a fashion identical to that seen in myeloid cells expressing endogenous MPO.

Figure 6. **Association of molecular chaperones with normal MPO in stably transfected HEK cells**
Stably transfected HEK cells expressing normal (wild-type MPO) or R499C mutant were biosynthetically radiolabeled for 1 hour and immunoprecipitated with anti-MPO or antibodies

against the molecular chaperones CRT, CLN, or ERp57 under nondenaturing conditions. Immunoprecipitates were analyzed by SDS-PAGE and autoradiography. Molecular chaperones coprecipitated with precursors of normal and mutant MPO (results representative of 3 independent experiments).

Figure 7. **Peroxidase activity of R499C MPO**
Wild-type HEK cells, HEK cells stably transfected with R499C or normal MPO (MPO), or purified MPO (2 μg) were separated in two identical native gels. Resultant gels were stained for peroxidase activity (panel A) or electroblotted to nitrocellulose and probed with anti-MPO (panel B). No peroxidase activity was identified in HEK cells or in R499C-HEK cells, whereas HEK-MPO cells exhibited peroxidase activity (panel A). The lack of activity in R499C-HEK cells did not reflect the absence of the mutant protein from the gel, as demonstrated by the presence of immunoreactive protein in the R499C-HEK cell immunoblot (panel B).

Figure 8. **Biosynthetic incorporation of heme into normal, R499C, and G501S MPO**
HEK transfectants expressing normal MPO (MPO), R499C, or G501S were pulse-labeled with [^{35}S]-methionine and chased 20 hours (A) or labeled with [^{14}C]-δ-aminolevulinic acid (B). The resultant cell lysates and culture media were immunoprecipitated with anti-MPO and analyzed by SDS-PAGE and autoradiography. Given the relative specific activities of the radioisotopes used, autoradiographs were exposed for 6 hours or 11 days for [^{35}S] and [^{14}C], respectively. Whereas heme was incorporated into the 90-kDa proMPO and 59-kDa mature subunit in HEK-MPO cells, heme acquisition for G501S and R499C was limited to the mutant 90-kDa proMPO form. When normalized for the amount of [^{35}S]-methionine labeled MPO precursor, heme incorporation for G501S and R499C was 23.7 ± 1.6 % and 28.7 ± 2.9 % of that for normal MPO. Values represent mean ± SEM, n =3.

Figure 9. **Spectral properties of normal and R499C MPO**
The 48,000 x g pellet recovered from wild-type HEK cells (WT) or from HEK cells stably expressing normal MPO (MPO) or the R499C mutant were scanned spectrophotometrically. Whereas pellets from wild-type HEK lysates lacked a Soret band, cells expressing normal MPO exhibited the ~430 nm peak characteristic of MPO. In contrast, the peak from R499C-HEK cells was shifted to 414 nm. Spectra are representative of 3 independent experiments.

Figure 1

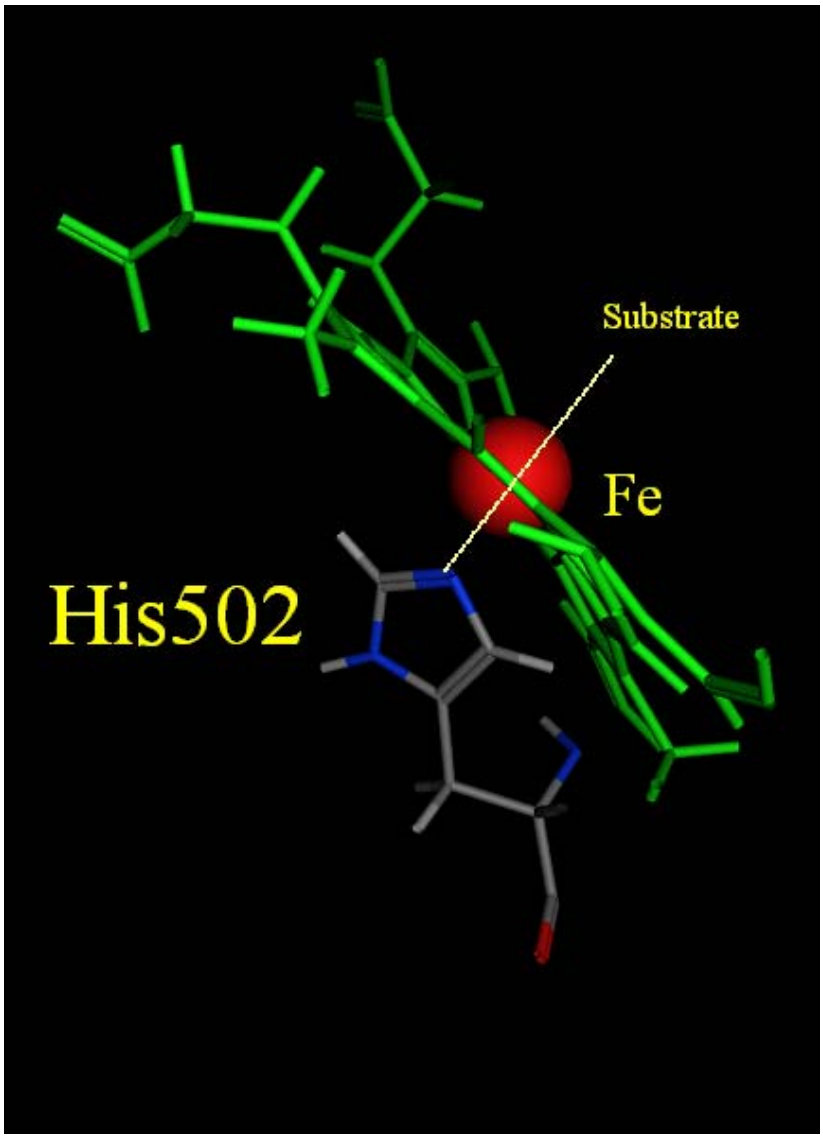

Figure 1B

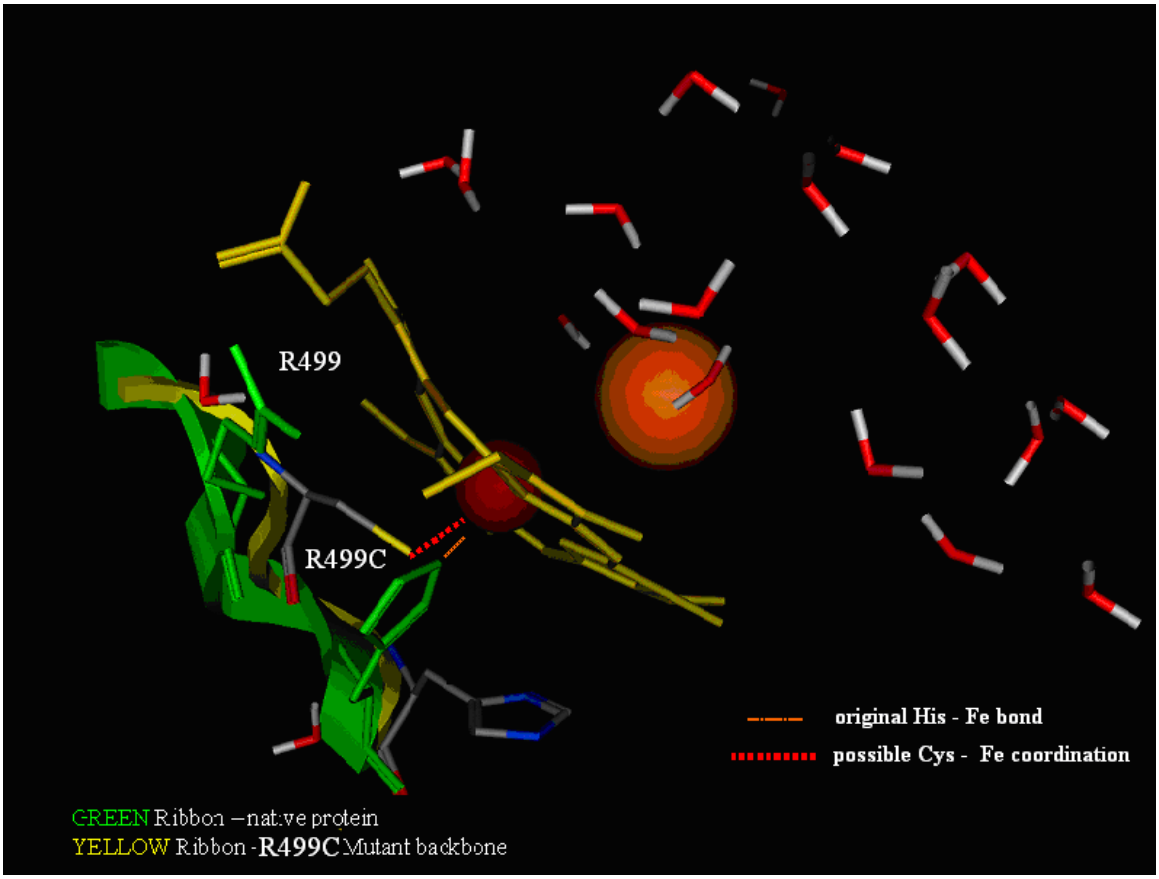

Figure 1C

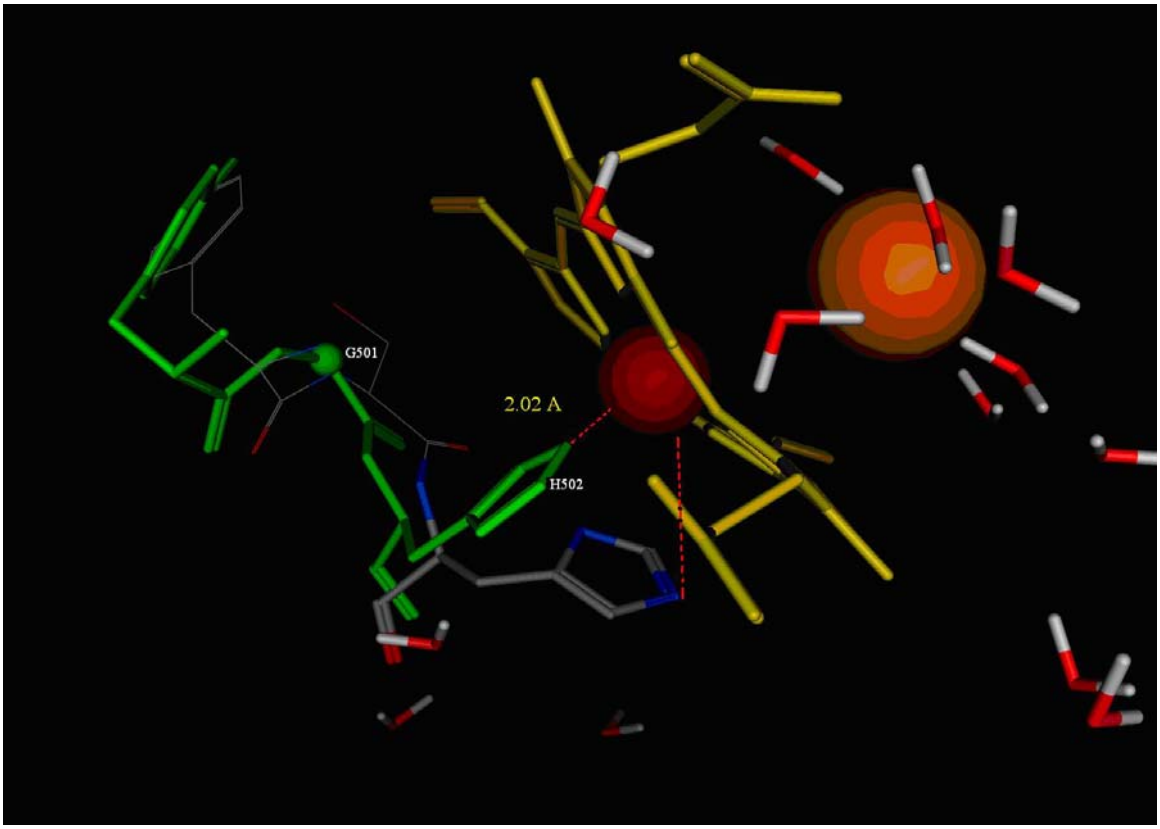

Figure 2

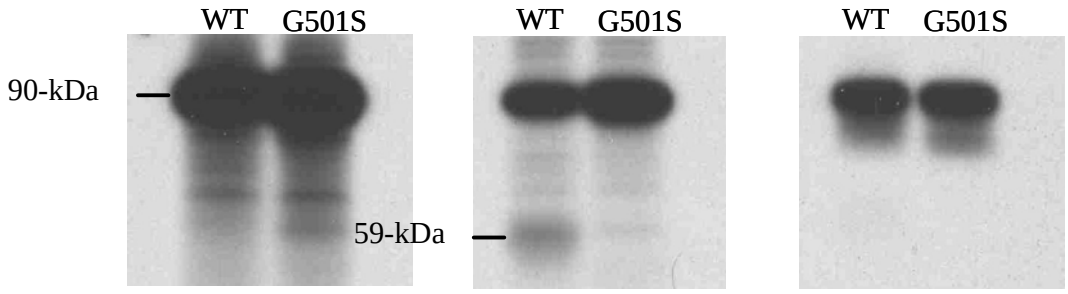

Cells : no chase Cells: 20 hrs chase Medium: 20 hrs chase

Figure 3

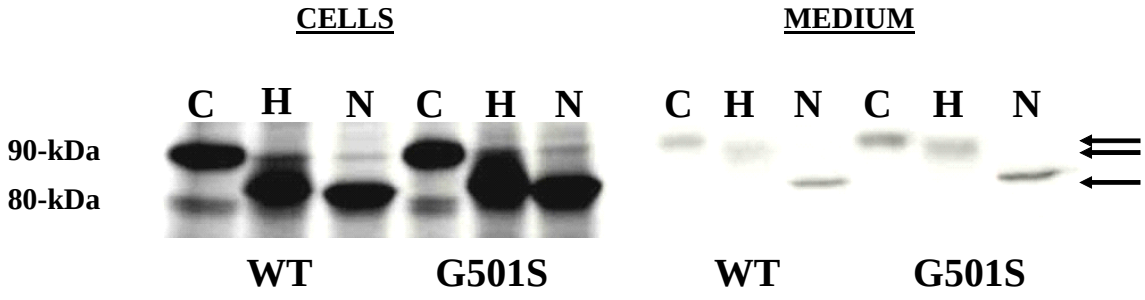

Figure 4

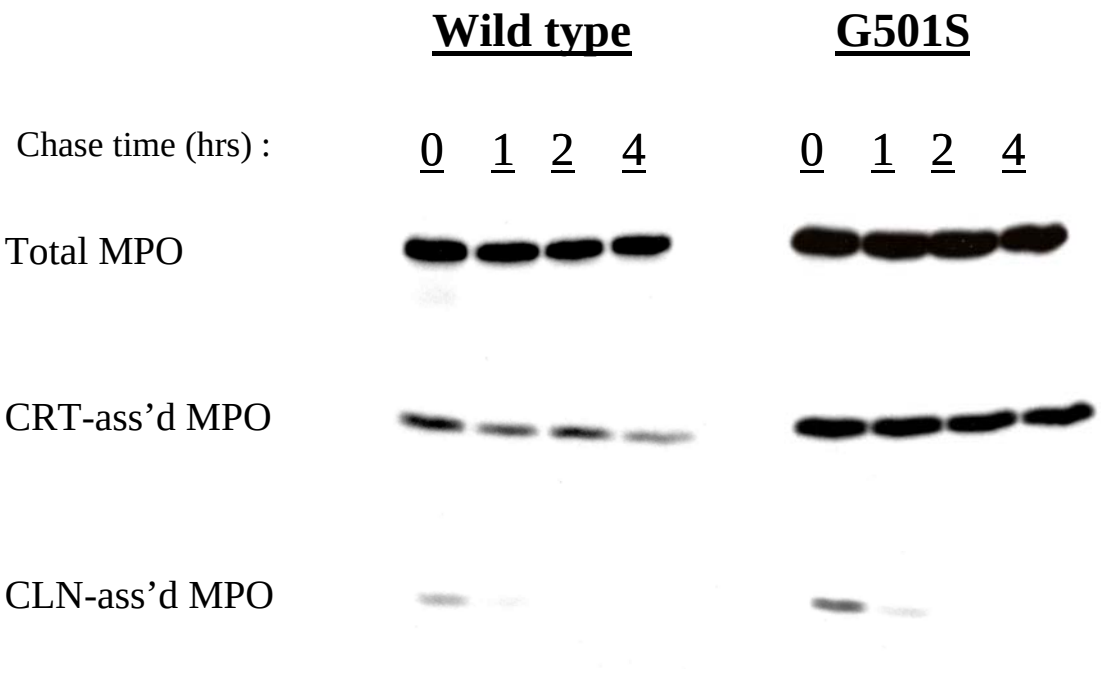

Figure 5

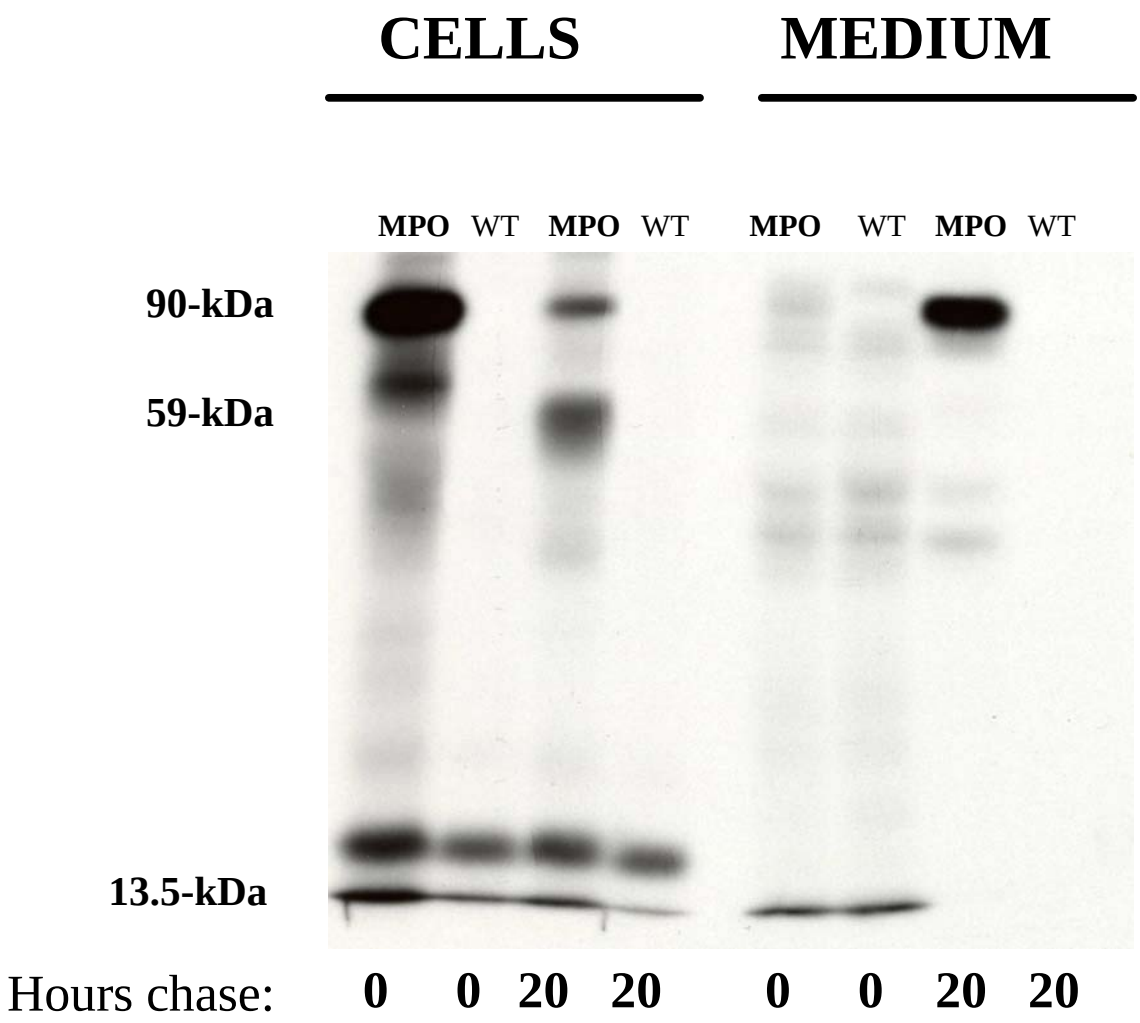

Figure 6

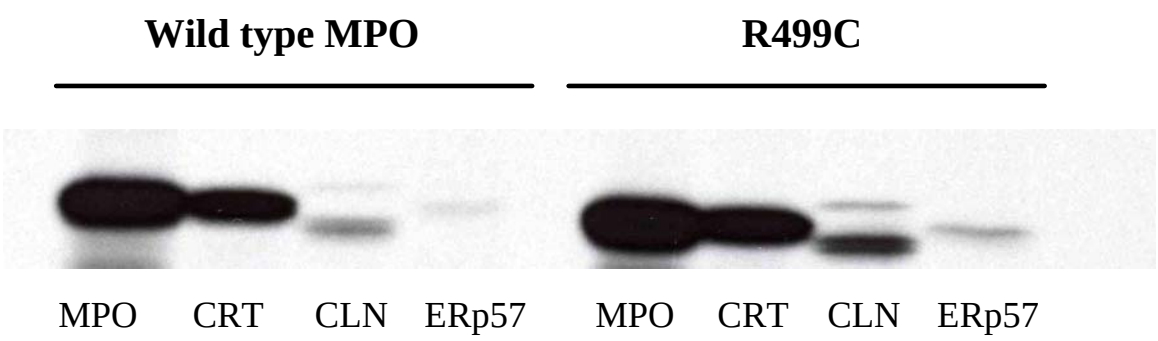

	MPO	R499C
CRT-associated	34.2%	33.6%
CLN-associated	4.6%	3.7%
ERp57-associated	1.9%	2.9%

Figure 7

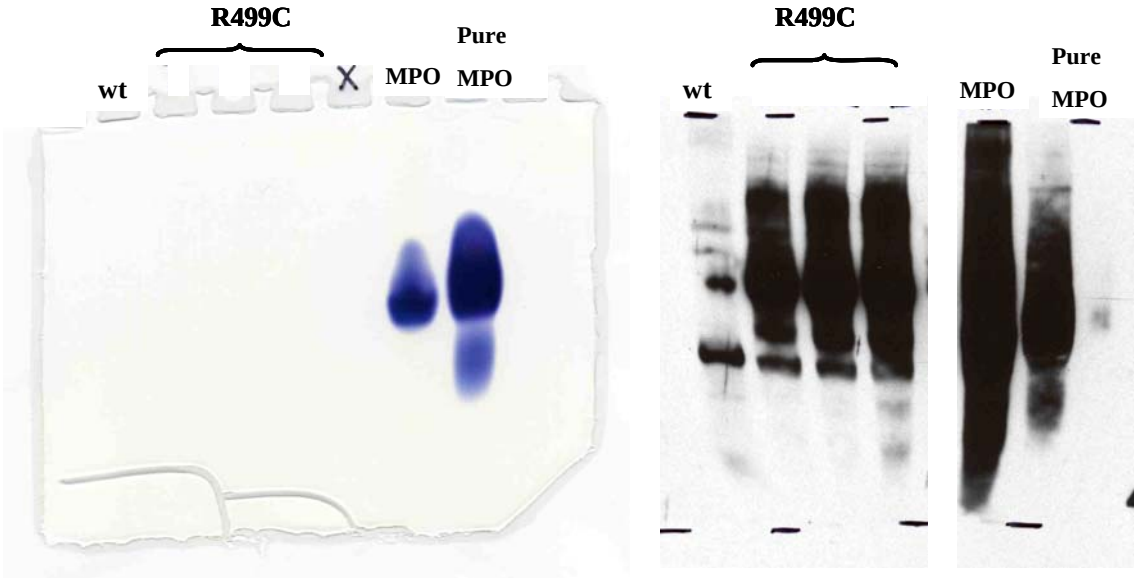

A) Native activity gel

B) Immunoblot of native gel

Figure 8

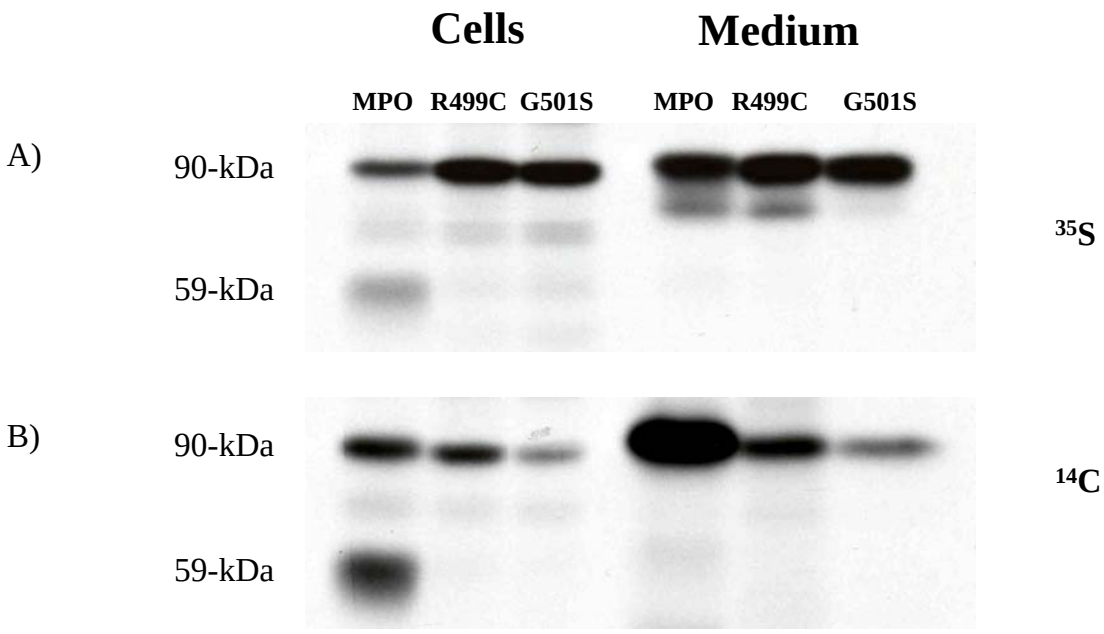

Figure 9

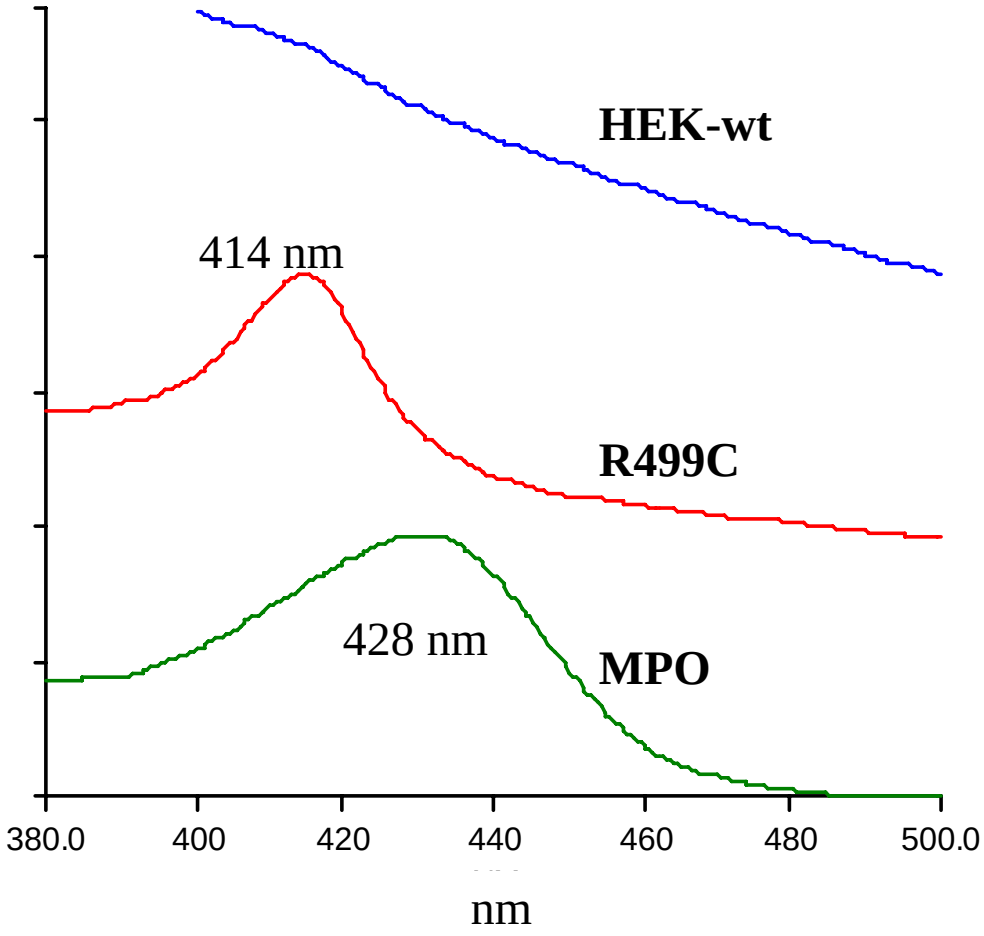

Impact of two novel mutations on the structure and function of human myeloperoxidase

Melissa Goedken, Sally McCormick, Kevin G. Leidal, Kazuo Suzuki, Yosuke Kameoka, Joshua M. Astern, Meilan Huang, Artem Cherkasov and William M. Nauseef

J. Biol. Chem. published online July 24, 2007 originally published online July 24, 2007
